IOSR Journal of Computer Engineering (IOSR-JCE)
e-ISSN: 2278-0661, p- ISSN: 2278-8727Volume 11, Issue 4 (May. - Jun. 2013), PP 27-36
www.iosrjournals.org

Performance Analysis of Rician Fading Channels using Non-linear Modulation Methods with Memory Schemes in Simulink environment

Sunil Kumar.P[#1], Dr.M.G.Sumithra[#2], Ms.M.Sarumathi[#3]
[#1] *P.G.Scholar, Department of ECE, Bannari Amman Institute of Technology, Sathyamangalam*
[#2] *Professor, Department of ECE, Bannari Amman Institute of Technology, Sathyamangalam*
[#3] *Assistant Professor, Department of ECE, Bannari Amman Institute of Technology, Sathyamangalam*

Abstract : *When a signal travels from transmitter to receiver over multiple reflective paths then the phenomenon is called as multipath propagation. In a wireless mobile communication system, the multipath propagation can cause the degradation in the received signal strength and this process is called as fading. When a strong stationary path such as a line of sight path is introduced into the Rayleigh fading environment, the fading becomes Rice-distributed fading. Ricean fading is utilized for characterizing satellite communications and in some urban environments. In this paper, the performance analysis of Ricean Fading Channels using Non-linear modulation methods with memory Schemes is implemented and the Bit Error Rate is analyzed using Simulink tool.*

Keywords - *Fading, Ricean, Non-linear, Memory, Simulink*

I. INTRODUCTION TO DIFFERENT TYPES OF CHANNEL FADING

There are usually three types of channel fading for mobile communications: shadowing (slow fading), multipath Rayleigh fading, and frequency-selective fading. Reflection, diffraction, and scattering are the three major mechanisms that influence the signal propagation.

1.1. Log-Normal Shadowing:

During the motion of an MS, clutter such as trees, buildings, and moving vehicles partially block and reflect the signal, thus resulting in a drop in the received power. In the frequency domain, there is a power decrease in a wide frequency range. Hence, it is called slow fading. The slow power variation relative to the average can be modelled by a log-normal probability function (pdf). For the log-normal distribution, the logarithm of the random variable has a normal distribution. The pdf and cumulative distribution function (cdf) are given by

$$\rho(r) = \frac{1}{r\sigma\sqrt{2\pi}} e^{-\frac{(\ln r - m)^2}{2\sigma^2}} \tag{1}$$

where m and σ are the mean and deviation, $P_r(.)$ is the probability function, and erf (x) is the well-known error function. In the shadowing model, the transmit-to-receive power ratio $\psi = \frac{P_t}{P_r}$ is assumed to be random with a log-normal distribution [1] and is expressed as follows

$$\rho(\psi) = \frac{10/\ln 10}{\sqrt{2\pi}\sigma_{\psi dB}\psi} \exp\left(-\frac{(\psi_{dB} - m_{\psi dB})^2}{2\sigma^2{}_{\psi dB}}\right), \psi > 0 \tag{2}$$

where $\psi_{dB} = 10\log_{10}\psi$ in decibels, and $m_{\psi dB,}\sigma_{\psi dB}$ are the mean and standard deviation of $\psi_{dB.}$. In this model, it is possible for ψ to t2ake on a value within 0 and 1, which corresponds to $P_r > P_{t,}$ but this is physically impossible. Nevertheless, this probability is very small when $m_{\psi dB}$ is a large and positive number. This fluctuation in mean power occurs on a large scale, typically dozens or hundreds of wavelengths, and thus, is also known as large-scale fading or macroscopic fading. Statistically, macroscopic fading is determined by the local mean of a fast fading signal. Trees cause an important class of environmental clutter. A tree with heavy foliage causes shadowing. A tree with full foliage in summer has approximately a 10 dB higher loss due to shadowing than the same tree without leaves in winter as it acts as a wave diffractor.

1.2. Rayleigh Fading:

When both the I and Q components of the received signal, x_I and x_Q normally distributed, the received signal is a complex Gaussian variable. The envelope of the received signal, $r = (x_I^2 + x_Q^2)^{1/2}$, is Rayleigh distributed, and r^2 has an exponential distribution. Note that the exponential distribution is a special case of the central- χ^2 distribution with m=1. The χ^2 distribution is the distribution of $Y=X^2$, where X is a Gaussian distribution. Assuming both x_I and x_Q have a standard deviation of σ, the total power in the received signal is $E[r^2]/2=\sigma^2$, and the pdfs is expressed by the following mathematical expression

$$\rho_r(r) = \frac{r}{\sigma^2} e^{-\frac{r^2}{2\sigma^2}}, 0 \le r < \infty \quad \text{and} \quad \rho_r{}^2(r) = \frac{1}{2\sigma^2} e^{-\frac{r}{2\sigma^2}} \tag{3}$$

For wireless communications, the envelope of the received carrier signal is Rayleigh distributed; such a type of fading is thus called Rayleigh fading. This can be caused by multipath with or without the Doppler effect. In the multipath case, when the dominant signal becomes weaker, such as in the non LOS case, the received signal is the sum of many components that are reflected from the surroundings. These independent scattered signal components have different amplitudes and phases (time delays); then the I and Q components of the received signal can be assumed to be independent zero-mean Gaussian processes. This is derived from the central limit theorem, which states that the sum of a sufficient number of random variables approaches very closely to a normal distribution.

1.3. Ricean Fading:

When a strong stationary path such as a LOS path is introduced into the Rayleigh fading environment, the fading becomes Rice-distributed fading. Ricean fading is suitable for characterizing satellite communications or in some urban environments. Ricean fading is also a small-scale fading. In this case, the probability of deep fades is much smaller than that in the Rayleigh-fading case. Based on the central limit theorem, the joint pdf of amplitude r and phase ϕ may be expressed as the following equation [2]

$$\rho_{r,\phi}(r,\phi) = \frac{r}{2\pi\sigma^2} e^{-\frac{r^2+A^2-2rA\cos\phi}{2\sigma^2}} \tag{4}$$

where A is the amplitude of the dominant component and σ is the same as that for Rayleigh fading,. This joint pdf is not separable, and the pdf of r or ϕ can be obtained by integrating over the other quantity. The pdf of the amplitude is a Rice distribution and is mathematically expressed as follows [3]

$$\rho_r(r) = \frac{r}{\sigma^2} e^{-\frac{r+A^2}{2\sigma^2}} I_0\left(\frac{rA}{\sigma^2}\right), 0 \le r < \infty \tag{5}$$

where $Z_0(x)$ is the modified Bessel function of the first kind and zero order, and is defined as follows

$$Z_0(x) = \frac{1}{2\pi} \int_0^{2\pi} e^{-x\cos\theta} d\theta \tag{6}$$

The mean square value of r is given by

$$\rho_r = 2\sigma^2 + A^2 \tag{7}$$

The Rice factor K*r* is defined as the ratio of the dominant component to the power in all the other components and it is given by the equation $K_r = \frac{A^2}{2\sigma^2}$ [4].The Rice distribution approximates the Rayleigh distribution with mean value A as Kr<<1, and reduces to it at Kr=0. It approximates the Gaussian distribution with mean value A as Kr>>1, and reduces to the Gaussian as $K_r \to \infty$.The factor Kr typically shows an exponential decrease with range, and varies from 20 near the BS to zero at a large distance. The dominant component changes the phase distribution from the uniformly random distribution of Rayleigh fading to clustering around the phase of the dominant component. The stronger the dominant component, the closer the resulting phase to the phase of the dominant component. This is similar to a delta function. Flat Ricean fading channel is suitable for characterizing a real satellite link.

1.4. Nakagami Fading:

The Nakagami distribution is another popular empirical fading model [5,6]

$$\rho(r) = \frac{2}{\Gamma(m)}(\frac{m}{2\sigma^2})^m r^{2m-1} e^{-m\frac{r^2}{2\sigma^2}}, r \geq 0 \tag{8}$$

Where $\sigma^2 = \frac{1}{2}E[r^2], \Gamma(.)$ is the Gamma function, and m $\geq 1/2$ is the fading figure. The received instantaneous power r^2 satisfies a Gamma distribution. The phase of the signal is uniformly distributed in [0,2π], which is independent of r. The Nakagami distribution is a general model obtained from experimental data fitting. The Nakagami distribution has a shape very similar to that of the Rice distribution. The shape parameter m controls the severity of fading. When m=1, the fading is close to Ricean fading, and the Nakagami and Rice distributions can approximate each other with the following mathematical expression,

$$K_r = (m-1) + \sqrt{m(m-1)}, m > 1 \tag{9}$$

$$m = \frac{(K_r + 1)^2}{2K_r + 1} \tag{10}$$

The Nakagami distribution has a simple dependence on r, and thus is often used in tractable analysis of fading performance [6]. When the envelope r is assumed to be Nakagami-distributed, the squared-envelope r^2 has a Gamma distribution [4]. The Nakagami distribution is capable of modeling more severe fading than Rayleigh fading by selecting ½ < m < 1. However, due to the lack of physical basis, the Nakagami distribution is not as popular as the Rayleigh and Ricean fading models in mobile communications.

1.5. Suzuki Fading:

The Suzuki model [7] is a statistical model that gives the composite distribution due to log-normal shadowing and Rayleigh fading. This model is particularly useful for link performance evaluation of slow moving or stationary MSs, since the receiver has difficulty in averaging the effects of fading. It is widely accepted for the signal envelope received in macro cellular mobile channels with no LOS path.

1.6. Doppler Fading:

Multipath components lead to delay dispersion, while the Doppler effect leads to frequency dispersion for a multipath propagation. Doppler spread is also known as time-selective spread. Frequency-dispersive channels are known as time-selective fading channels. Signals are distorted in both the cases. Delay dispersion is dominant at high data rates, while frequency dispersion is dominant at low data rates. The two dispersions are equivalent, since the Fourier transform can be applied to move from the time domain to the frequency domain. These distortions cannot be eliminated by just increasing the transmit power, but can be reduced or eliminated by equalization or diversity.

II. A Review On The Wide Sense Stationary Uncorrelated Scattering Model

Wireless channels are time-variant, with an impulse response h (t,τ), and can be modelled by using the theory of linear time-variant systems. Because most wireless channels are slowly time-varying, or quasi-static, this enables the use of many concepts of linear time-invariant (LTI) systems. By performing the Fourier transform to the absolute time t, or the delay τ, or both, we obtain the delay Doppler-spread function S (v,τ), the time-variant transfer function H(t,f), or the Doppler-variant transfer function B(v,f), respectively. The stochastic model of wireless channels is a joint pdf of the complex amplitudes for any τ and t. The ACF is usually used to characterize the complex channel. The ACF of the received signal, y(t)=x(t) * h(t,τ), for a linear time-variant system is given by

$$R_{yy}(t,t') = \int_{-\infty}^{\infty}\int_{-\infty}^{\infty} R_{xx}(t-\tau, t'-\tau') R_h(t,t',\tau,\tau') d\tau d\tau' \tag{11}$$

where the ACFs are

$$R_{XX}(t-\tau, t'-\tau') = E[x^*(t-\tau)x(t'-\tau')] \tag{12}$$

$$R_h(t,t',\tau,\tau') = E[h^*(t,\tau)h(t',\tau')] \tag{13}$$

A stochastic process is said to be strictly stationary if all its statistical properties are independent of time. When only the mean is independent of time while the autocorrelation depends on the time difference $\Delta t = t' - t$, such a process is said to be a wide sense stationary process. The popular WSSUS (wide sense stationary, uncorrelated

scattering) model is based on the dual assumption: wide sense stationarity and uncorrelated scatters. The assumptions of wide sense stationarity states that the ACF of the channel is determined by the difference Δt, that is,

$$R_h(t,t',\tau,\tau') = R_h(\Delta t,\tau,\tau') \tag{14}$$

Thus, the statistical properties of the channel do not change over time, and the signals arriving with different Doppler shifts are uncorrelated

$$R_h(v,v',\tau,\tau') = P_s(v,\tau,\tau')\delta(v-v') \tag{15}$$

where P_s the scattering function, giving the Doppler power spectrum for a multipath channel with different path delays τ.

2.1. Delay Spread:

The delay power spectral density or power delay profile (PDP), $P_h(\tau)$, is obtained by integrating the scattering function $P_s(\tau,v)$ over the Doppler shift v. The PDP can be calculated by the following expression

$$P_h(\tau) = \sum_{n=1}^{N} P_n \delta(\tau-\tau_n) = \int_{-\infty}^{\infty} \left| h(t,\tau) \right|^2 dt \tag{16}$$

where $P_n = a_n^2$, a_n being the amplitude of the nth delay, and the second equality holds if ergodicity holds. First arrival delay τ_A is the delay of the first arriving signal, all the other delays are known as excess delays, and the maximum excess delay τ_{max} is the delay corresponding to a specified power threshold. Delay spread leads to frequency-selective fading, as the channel function resembles a tapped-delay filter. A general rule of thumb is that $\tau_{max} \approx 5\sigma_\tau$. The PDP has been modelled in order to understand the channel behaviour and to evaluate the performance of equalizers. There are many measurements of indoor and outdoor channels [8]. The one-sided exponential profile is a suitable model for both indoor and urban channels

$$P_h(\tau) = \frac{P_T}{\sigma_\tau} e^{-\frac{\tau}{\sigma_\tau}}, \tau \geq 0 \tag{17}$$

where P_T is the total received power. When the excess delay spread exceeds the symbol duration by 10% to 20%, an equalizer may be required. The average delay and the delay spread of a channel diminish with decreasing cell size due to shorter propagation path.

2.2 Correlation Coefficient:

The correlation coefficient of two signals is usually defined with respect to the signal envelopes x and y

$$\rho = \rho_{xy} = \frac{E[xy]-E[x]E[y]}{\sqrt{(E[x^2]-E[x]^2)(E[y^2]-E[y]^2)}} \tag{18}$$

For two statistically independent signals, ρ=0; when ρ is below a threshold such as 0.5, the signals are typically considered effectively as decorrelated. For a channel with PDP of type (16), assuming a classical Doppler spectrum for all the components, the correlation coefficient of two signals with a temporal separation Δt and a frequency separation Δf is given by [9, 2]

$$\rho_{xy}(\Delta t,\Delta f) = \frac{J_0^2(2\pi v_{max}\Delta t)}{1+(2\pi\sigma_\tau\Delta f)^2} \tag{19}$$

where $J_0(x)$ is the zero-order Bessel function of the first kind and v_{max} is the maximum Doppler frequency.

2.3. Channel Coherent Bandwidth:

The channel coherence bandwidth B_c is defined as the maximum frequency difference $(\Delta f)_{max}$ that limits the correlation coefficient ρ to be smaller than a given threshold, typically 0.7 is given as follows

$$B_c = (\Delta f)_{max} = \frac{1}{2\pi\sigma_\tau} \tag{20}$$

Due to the uncertainty relation between the Fourier transform pairs, there is an uncertainity relation between B_c and the rms relay spread σ_τ [2] as follows

$$B_c \geq \frac{1}{2\pi\sigma_\tau} \tag{21}$$

That is, both B_c and σ_τ can be used to characterize the channel, and they are in inverse proportion; although usually they can be related by the approximation $B_c \approx \frac{1}{\sigma_\tau}$, they cannot be exactly derived from each other.

2.4. Doppler Spread And Channel Coherent Time:

The Doppler power spectral density $P_B(v)$ is obtained by integrating the scattering function $P_s(\tau,v)$ over the time delay τ. Analogous to the derivation of the average channel delay $\bar{\tau}$ and rms delay spread σ_τ can be derived as the first- and second-order moments of $P_B(v)$. The Doppler spread corresponds to time-selective fading. The channel coherence time T_c is also defined according to (19). The coherent time measures how fast the channel changes in time. A large coherent time corresponds to a slow channel fluctuation. The coherence time is defined in a manner similar to that of the coherent bandwidth. It is defined as the time delay for which the signal autocorrelation coefficient reduces to 0.7.

2.5. Angle Spread And Coherent Distance:

The channel model can also include the directional information such as the DoA and DoD of the multipath components into its impulse response, leading to the double-directional impulse response. Analogous to the non directional case, a number of power spectrums such as the double directional delay power spectrum, angular delay power spectrum, angular power spectrum, and azimuthal spread can be defined [10]. Such a directional channel model is especially useful for multiple antenna systems. Angle spread at the receiver is the spread in DoA of the multipath components at the receive antenna array, while angle spread at the transmitter is the spread in DoDs of the multipath components that finally arrive at the receiver. Denoting the DoA by Θ, the angle power spectrum or power angular profile $P_A(\Theta)$ is given by the following expression

$$P_A(\theta) = \sum_{n=1}^{N} P_n \delta(\theta - \theta_n) \tag{22}$$

III. Non-Linear Modulation Methods With Memory-Cpfsk And Cpm

A class of digital modulation methods in which the phase of the signal is constrained to be continuous. This constraint results in a phase or frequency modulator that has memory. The modulation method is also non-linear.

3.1. CONTINUOUS-PHASE FSK (CPFSK): An conventional FSK signal is generated by shifting the carrier by an amount $f_n = \frac{1}{2}\Delta f I_{n,} I_n = \pm 1, \pm 3, ..., \pm(M-1),$ to reflect the digital information that is being transmitted. The switching from one frequency to another may be accomplished by having $M=2^k$, separate oscillators tuned to the desired frequencies and selecting one of the M frequencies according to the particular k-bit symbol that is to be transmitted in a signal interval of duration T=k/R seconds. However, such abrupt switching from one oscillator output to another in successive signaling intervals results in relatively large spectral side lobes outside the main spectral band of the signal and, consequently, this method requires a large frequency band for transmission of the signal.

To avoid the use of signals having large spectral side lobes, the information-bearing signal frequency modulates a single carrier whose frequency is changed continuously. The resulting frequency-modulated signal is phase-continuous and, hence, it is called continuous-phase FSK (CPFSK)[11]. This type of FSK signal has memory because the phase of the carrier is constrained to be continuous. In order to represent a CPFSK signal, we begin with a PAM signal and it is expressed as follows

$$d(t) = \sum_n I_n g(t - nT) \tag{23}$$

where $\{I_n\}$ denotes the sequence of amplitudes obtained by mapping k-bits blocks of binary digits from the information sequences $\{a_n\}$ into the amplitudes levels $\pm 1, \pm 3, ..., \pm(M-1)$ and g(t) is a rectangular pulse of x amplitude 1/2T and duration T seconds. The signal d(t) is used to frequency-modulate the carrier. Consequently, the equivalent low-pass waveform v(t) is expressed as follows

$$v(t) = \sqrt{\frac{2\varepsilon}{T}} \exp\{ j\left[4\pi T f_d \int_{-\infty}^{t} d(\tau) d\tau + \phi_0 \right]\} \tag{24}$$

where f_d is the peak frequency deviation and ϕ_0 is the initial phase of the carrier. The carrier-modulated signal corresponding to the (24) may be expressed as the following

$$s(t) = \sqrt{\frac{2\varepsilon}{T}} \cos[2\pi f_c t + \phi(t;I) + \phi_0] \tag{25}$$

$$\text{where } \phi(t;I) = 4\pi T f_d \int_{-\infty}^{t} d(\tau) d\tau$$

$$\phi(t;I) = 4\pi T f_d \int_{-\infty}^{t} [\sum_n I_n g(\tau - nT)] d\tau \tag{26}$$

It is noted that, although d(t) is contains discontinuities, the integral of d(t) is continuous. Hence, we have a continuous-phase signal. The phase of the carrier in the interval $nT \le t \le (n+1)T$ is determined by integrating (26). Thus the following equations are obtained

$$\phi(t;I) = 2\pi f_d T \sum_{k=-\infty}^{n-1} I_k + 2\pi f_d (t - nT) I_n \tag{27}$$

$$= \theta_n + 2\pi h I_n q(t - nT) \tag{28}$$

Where h, Θ_n, and q(t) are defined as

$$h = 2 f_d T \tag{29}$$

$$\theta_n = \pi h \sum_{k=-\infty}^{n-1} I_k \tag{30}$$

$$q(t) = \begin{cases} 0 \; for (t < 0) \\ t / 2T for (0 \le t \le T) \\ 1/2 \; for (t > T) \end{cases} \tag{31}$$

The observation is that Θ_n represents the accumulation (memory) of all symbols up to time (n-1) T. The parameter h is called the modulation index.

3.2. CONTINUOUS-PHASE MODULATION (CPM):

When expressed in the form of (28), CPFSK becomes a special case of a general class of continuous-phase modulated (CPM) signals in which the carrier phase is written as follows:

$$\phi(t;I) = 2\pi \sum_{k=-\infty}^{n} I_k h_k q(t - kT), nT \le t \le (n+1)T \tag{32}$$

Where $\{I_k\}$ is the sequence of M-ary information symbols selected from the alphabet $\pm 1, \pm 3, ... \pm (M-1)$, $\{h_k\}$ is a sequence of modulation indices, and q(t) is some normalized waveform shape. When h_k=h for all k, the modulation index is fixed for all symbols. When the modulation index varies from one symbol to another, the CPM signal is multi-h. In such a case, the $\{h_k\}$ are made to vary in a cyclic manner through a set of indices. The waveform q(t) may be represented in general as the integral of some pulse g(t), i.e.,

$$q(t) = \int_0^t g(\tau) d\tau \tag{33}$$

If g(t)=0 for t>T, the CPM signal is called full response CPM. If $g(t) \neq 0$ for t>T, the modulated signal is called partial response CPM. It is apparent that an infinity variety of CPM signals can be generated by choosing different pulse shapes g(t) and by varying the modulation index h and the alphabet size M. It is noted that the CPM signal has memory that is introduced through the phase continuity [12]. For L>1, additional memory is introduced in the CPM signal by the pulse g(t) and by varying the modulation index h and the alphabet size M.

IV. Performance Analysis Of Rician Fading Channels Using Cpfsk And Cpm In Simulink:

The environment is created as shown in the fig. 1.and fig.2. respectively using Simulink tool.

5.1 RANDOM INTEGER GENERATOR: The random integer generator generates random uniformly distributed integers in the range [0, M-1], where M is the M-ary number.

5.2. INTEGER TO BIT CONVERTER: In the integer to bit convertor unit, a vector of integer-valued or fixed valued type is mapped to a vector of bits. The number of bits per integer parameter value present in the integer to bit convertor block defines how many bits are mapped for each integer-valued input. For fixed-point inputs, the stored integer value is used. This block is single-rated and so the input can be either a scalar or a frame-based column vector. For sample-based scalar input, the output is a 1-D signal with 'Number if bits per integer' elements. For frame-based column vector input, the output is a column vector with length equal to 'Number of bits per integer' times larger than the input signal length.

5.3 DIFFERENTIAL ENCODER: Differential encoder differentially encodes the input data. The differential encoder object encodes the binary input signal within a channel. The output is the logical difference between the current input element and the previous output element.

5.4 CONVOLUTIONAL INTERLEAVER: This block permutes the symbols in the input signal. Internally, it uses a set of shift registers. The delay value of the kth shift register is (k-1) times the register length step parameter. The number of shift registers is the value of the rows of shift registers parameter.

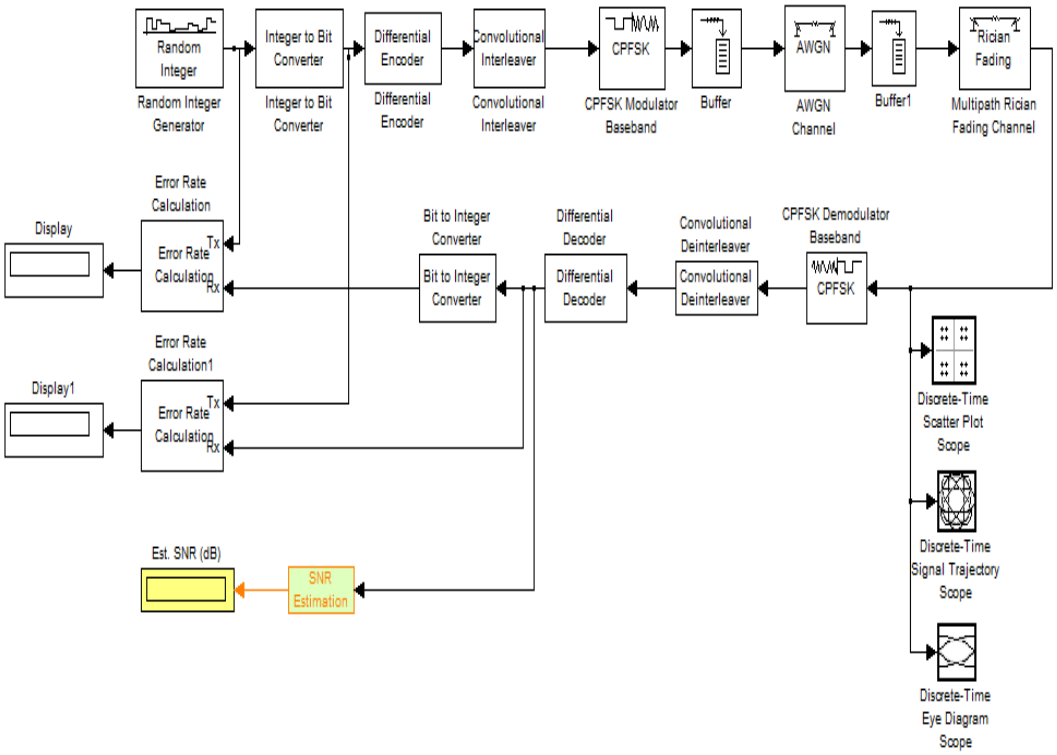

Fig. 1. Screenshot for the performance analysis of Rician fading channels using CPFSK modulation in Simulink

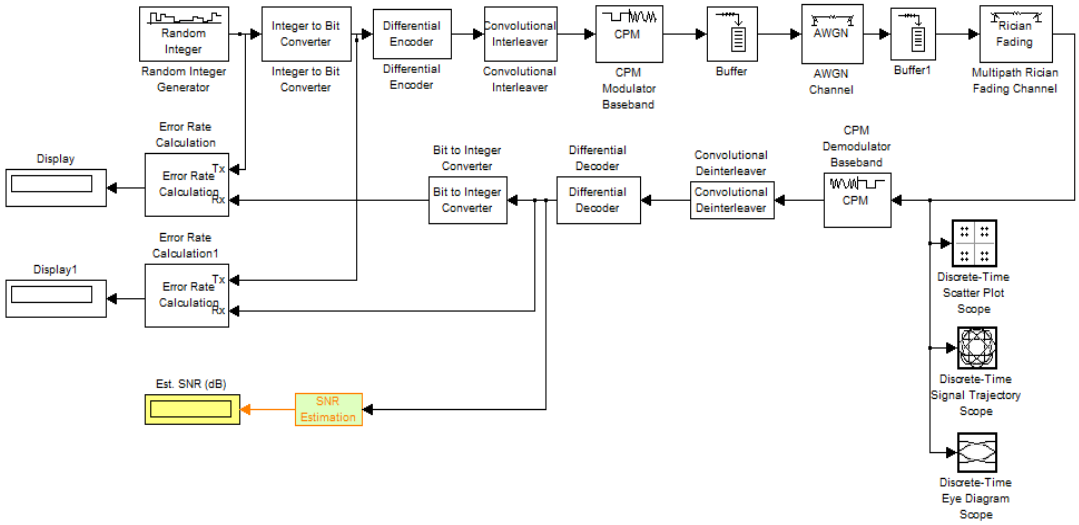

Fig. 2. Screenshot for the performance analysis of Rician fading channels using CPM modulation in Simulink

5.5 CPFSK MODULATOR BASEBAND: This block modulates the input signal using the continuous phase frequency shift keying method. The input can be either bits or integers.
5.6.CPFSK DEMODULATOR BASEBAND: This block demodulates the CPFSK modulated input signal using the Viterbi algorithm.
5.7 CPM MODULATOR BASEBAND: This block gives the output of the complex envelope representation of the selected continous phase modulation. The input can be either bits or integers.
5.8 CPM DEMODULATOR BASEBAND: This block demodulates the CPM modulated input signal using the Viterbi algorithm.
5.7 BUFFER: The buffer converts scalar samples to a frame output at a lower sample rate. The conversion of a frame to a larger size or smaller size with optional overlap is possible. It is then passed to the multipath Rician fading channel.
5.8 CONVOLUTIONAL DEINTERLEAVER: The Convolutional deinterleaver block recovers a signal that was interleaved using the Convolutional interleaver block.
5.9 DIFFERENTIAL DECODER: The differential decoder block decodes the binary input signal.
5.10 BIT TO INTEGER CONVERTER: The bit to integer converter maps a vector of bits to a corresponding vector of integer values. The number of bits per integer parameter defines how many bits are mapped for each output.
5.11 ERROR RATE CALCULATION: The error rate calculation is done by computing the error rate of the received data by comparing it to a delayed version of the transmitted data.
5.12 SIGNAL TRAJECTORY SCOPE: The discrete-time signal trajectory scope is used to display a modulated signal constellation in its signal space by plotting the in phase component versus the quadrature component.
5.13 SCATTER PLOT SCOPE: The discrete-time scatter plot scope is used to display a modulated signal constellation in its signal space by plotting the in phase component versus the quadrature component.
5.14 EYE DIAGRAM SCOPE: The discrete-time eye diagram scope displays multiple traces of a modulated signal to reveal the modulation characteristics such as pulse shaping, as well as channel distortions of the signal.
5.15 SNR ESTIMATION: The SNR estimation block gives the estimated SNR in decibels.
5.16 DISPLAY: This unit gives the total number of bits transmitted, the number of errors and finally displays the Bit Error Rate.

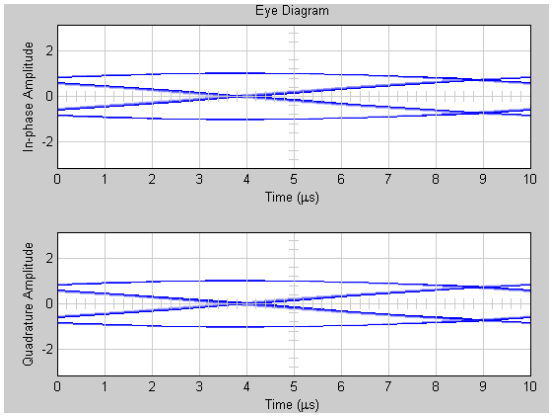

Fig. 1.Eye diagram for the performance analysis of Rician Fading Channels in CPFSK scheme

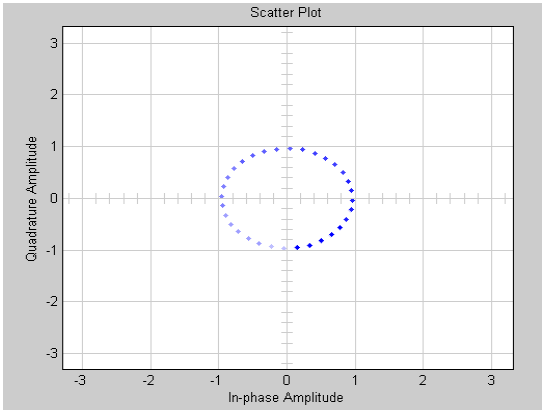

Fig. 2. Scatter plot for the performance analysis of Rician Fading Channels in CPFSK scheme

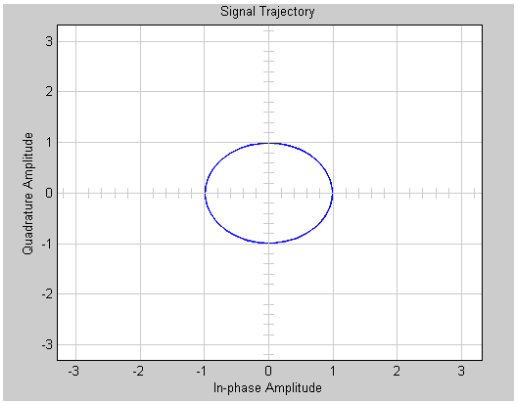

Fig. 3. Signal Trajectory for the performance analysis of Rician Fading Channels in CPFSK scheme

Table.1. BER for Rician fading channels in CPFSK modulation scheme

K_r(Ricean factor)	SNR(dB)	BER
100	10	0.009079
500	50	0.009048
1000	100	0.008895

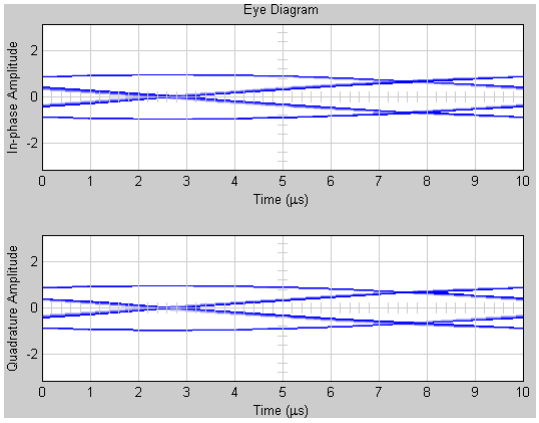

Fig. 4. Eye diagram for the performance analysis of Rician Fading Channels in CPM scheme

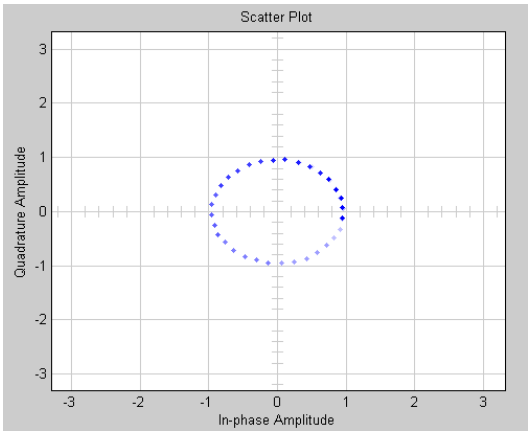

Fig. 5. Scatter plot for the performance analysis of Rician Fading Channels in CPM scheme

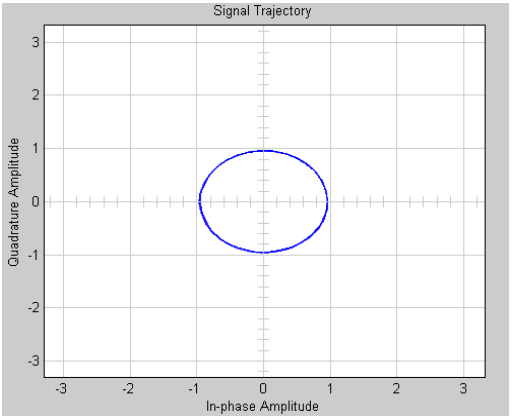

Fig. 6. Signal Trajectory for the performance analysis of Rician Fading Channels in CPM scheme

Table.2. BER for Rician fading channels in CPM schemes

K_r(Ricean factor)	SNR(dB)	BER
100	10	0.009317
500	50	0.009288
1000	100	0.009126

V. Conclusion

A short survey on different types of channel fading is provided followed by a review on wide sense stationary uncorrelated scattering model. The analysis of Rician fading channels in CPFSK modulation schemes and CPM modulation schemes is discussed and the results are provided. It is evident from table 1 and table 2 that when the Ricean factor (K_r) and the Signal-to-Noise Ratio is increased then the resulting Bit Error Rate gradually decreases. For high values of K_r, a very low bit error rate is achieved in CPFSK modulation scheme than in the CPM modulation scheme. The eye diagram, signal trajectory diagram and the scatter plot diagrams have also been provided for the scenario. Future works may include finding the bit error rate by evaluating the performance of Rician fading channels by using various modulation schemes and by altering the Ricean factor parameters.

References:

[1] A.Goldsmith, *Wireless Communication* (Cambridge, UK:Cambridge University Press,2005)
[2] A.F.Molisch, *Wireless Communications* (Chichester: Wiley-IEEE,2005).
[3] S.O.Rice, Statistical properties of a sine wave plus random noise. *Bell Syst.Tech.J.*, 27:1 (1948), 109-157.
[4] G.L.Stuber, *Principles of Mobile Communication*, 2nd edn (Boston, MA:Kluwer, 2001).
[5] M.Nakagami, The m-distribution: a general formula of intensity distribution of rapid fading. In W.C.Hoffman, ed., *Statistical Methods in Radio Wave Propagation* (Oxford:Pergamon Press, 1960), pp.3-36.
[6] M.K.Simon and M.-S.Alouini, *Digital Communications over Fading Channels*, 2nd edn (New York: Wiley, 2005).
[7] H.Suzuki, A statistical model for urban radio propagation, *IEEE Trans. Commun*., 25:7 (1977), 673-680.
[8] J.Chuang, The effects of time delay spread on portable radio communications channels with digital modulation. *IEEE J.Sel.Areas.Commun*., 5:5(1987), 879-889.
[9] W.C.Jakes, Jr. (ed.), *Microwave Mobile Communications* (New York: Wiley, 1974).
[10] B.H.Fleury, First- and second-order characterization of direction dispersion and space selectivity in the radio channel. *IEEE Trans. Inf.Theory*, 46:6 (2000), 2027-2044.
[11] J.M.Wozencraft and I.M.Jacobs, *Principles of Communication Engineering*, Wiley, New York 1965.
[12] C.R.Cahn, "Combined Digital Phase and Amplitude Modulation Communication Systems," *IRE Transactions on Communications Systems*, Vol. CS-8, pp.150-154, 1960.